One Nanosecond Photon Correlation Spectroscopy on Smectic Liquid Crystal Films

S. Sharma, K. Neupane, A. Adorjan, A. R. Baldwin, and S. Sprunt
Department of Physics, Kent State University, Kent, Ohio 44242 USA
(Received 15 October 2004; published 17 February 2005)

We have extended photon correlation spectroscopy down to a one-nanosecond time scale, and applied it to a study of layer undulations in freestanding smectic-*A* films of two cyanobiphenyl liquid crystals. Temporal correlations in the intensity of scattered light reveal an interesting combination of under- and overdamped modes. The underdamped mode is accurately described by a recently calculated correlation function of the smectic layer displacement, although its frequency and damping rate exhibit stronger dispersion at large optical wave vectors than expected from current dynamical models for smectic films.

DOI: 10.1103/PhysRevLett.94.067801 PACS numbers: 61.30.Eb, 61.30.Cz, 78.35.+c

The dynamics of fluid molecular membranes are a fundamentally significant problem in condensed matter physics, impacting our understanding of phenomena ranging from ordering and self-assembly of soft materials all the way to biological processes in living cells. Despite decades of development of the hydrodynamic theory of these systems, light scattering experiments on membrane fluctuations in one of the most basic cases—thermotropic smectic liquid crystal films—have been mainly confined to either frequency domain measurements above $\sim$1 GHz, which probe sound waves in a limit where damping is a weak effect [1], or photon correlation spectroscopy (PCS) studies that are carried out in the time domain (typically below 10 MHz or for times $\gtrsim 0.1$ μsec), and usually designed to study overdamped fluctuations of the smectic layer orientation when inertia is negligible [2,3]. The interesting crossover regime, where inertia, damping, and elastic forces all contribute significantly in the hydrodynamic description, has proved quite challenging for scattering experiments.

In this Letter, we report an extension of optical PCS down to 1 ns resolution, which allows us to determine both the propagation frequency and damping rate for undulatory motion of films as thin as a few tens of molecular layers and out to in-plane wave vectors near the optical limit ($q_\perp \sim 10^5$ cm^{-1}). Our work substantially builds on a previous light beating study performed in the frequency domain [4], and on recent results of elegant synchrotron x-ray PCS [5–7] and neutron spin echo [7] studies, by providing new detail about the dispersion in $q_\perp$ of the undulation mode and about the crossover from under- to overdamped dynamical behavior. We focus on freely suspended smectic-*A* films of two cyanobiphenyl compounds, 8CB and 9CB. The smectic layering in such films is essentially ideal, with the equilibrium layer planes parallel to the film surfaces. In thinner films and for sufficiently small $q_\perp$, we find that the measured time correlation functions of fluctuations in the layer displacement (u), as well as the resulting $q_\perp$ dependence of the frequency and damping associated with these fluctuations, are described well by the available predictions from the hydrodynamic theory [5–10]. However, this agreement fails at large $q_\perp$, in part because the effective viscosity for undulations of our smectic-*A* films is apparently quite small—at least 10 times lower than values of individual smectic viscosities previously determined for bulk samples [11,12]—even though the key static parameter (the film surface tension) is consistent with prior measurements [13]. As a consequence, higher order terms in the dispersion relations for u fluctuations are needed to model the experimental results. Our data also reveal an additional purely overdamped mode that contributes even for values of $q_\perp$ where the correlation functions are dominated by film undulations that are clearly underdamped.

To measure time correlation functions accurately at nanosecond delays, we designed and constructed a digital electronic correlator that records photo-pulse arrival times down to 0.5 nsec from two separate photomultipliers (A and B), and computes the time cross-correlation function $[\langle A(0)B(\tau)\rangle + \langle B(0)A(\tau)\rangle]/2$ with the following channel layout: 32 768 1 nsec channels that can be flexibly binned to produce longer time intervals, plus 8 sets of 128 channels spaced by each of the fixed intervals 1, 10, and 100 μ sec, 1, 10, and 100 msec, and 1 and 10 sec [14]. The scattered light was split between the two photomultipliers, which have nanosecond rise times. We also constructed special amplifier-discriminator circuits with two thresholds to establish a timing reference on the photopulses as well as a pulse acceptance level. A high speed, precision pulsed light-emitting diode, which generates a sharply spiked correlation function, was used to calibrate zero delay time.

Freestanding smectic films were drawn across a 7 mm diameter hole in a polished stainless steel substrate and housed in a specially modified, sealed microscope hot stage, which was then mounted onto a two-circle goniometer. The film thickness was continuously monitored by optical reflectivity. The center of the film was illuminated, at an incident angle of 27.3° with respect to the horizontal film normal, by a focused 532 nm laser beam, which had a vertical (ordinary) polarization and a power between 1.2 and 80 mW. Scattering of the same (ordinary) polarization

 © 2005 The American Physical Society

was collected at various angles off the specular reflection [15]. Because the $o - o$ polarized scattering is overwhelmingly due to modulations in the surface reflectivity produced by undulations of the film, the measured time correlation function of the scattered intensity can be directly related to correlations of the layer displacement evaluated at the surfaces [16].

Figs. 1 and 2 show typical correlograms measured for various $q_\perp$ on 90 nm thick 9CB and 240 nm thick 8CB films in the homodyne limit. Additional data (not shown) were collected from 230 nm 9CB and 100 nm 8CB films. For the 9CB films, the temperature was approximately 0.5 °C below the smectic-A to nematic transition, while the measurements on 8CB films were taken 7 °C below the transition. With increasing $q_\perp$, both the oscillation period and the damping time characterizing the underdamped behavior of the data clearly shift to lower τ. At large $q_\perp$ in the thicker films, we also observe an apparent crossover to overdamped fluctuations. In the underdamped regime, the data reveal more complicated behavior than anticipated for a single mode. Specifically, there is evidence of beating with an additional mode: At intermediate $q_\perp$, the peak height of the oscillations alternates as a function of τ for the thinner film (Fig. 1), while for the thicker film (Fig. 2), the oscillations can also be seen to "ride" on top of the decay of an additional mode.

In order to analyze our data quantitatively, we consider the layer displacement correlation function that has been calculated by Chen and Jasnow [10] for the case of an incompressible, isothermal smectic film. In this limit, taking z as the layer normal, one finds a pair of modes coupling the "transverse" component of the molecular velocity $v_t \equiv (q_\perp v_z - q_z v_\perp)/q$ to the smectic layer displacement u. The resulting layer correlation function $C_u(\tau) \equiv \langle u^*(0)u(\tau)\rangle$ may be expressed as [10]

$$C_u(\tau) = C_0 e^{-\Gamma\tau}\cos[\sqrt{\Omega}\tau - \tan^{-1}(\Gamma/\sqrt{\Omega})](\Omega > 0) \quad (1a)$$

$$C_u(\tau) = C_+ e^{-\Gamma_+\tau} + C_- e^{-\Gamma_-\tau}(\Omega < 0). \quad (1b)$$

Here $\Gamma = [\eta_3\vec{q}^2 + \eta' q_\perp^2 q_z^2/\vec{q}^2 + \rho\lambda_P^2(Bq_z^2 + Kq_\perp^4)/\eta_3]/2\rho$, $\Omega = (Bq_z^2 + Kq_\perp^4)[q_\perp^2 + \lambda_P^2(\vec{q}^4 + \eta' q_\perp^2 q_z^2/\eta_3)]/(\rho\vec{q}^2) - \Gamma^2$, and $\omega = \sqrt{|\Omega|}$ for $\Omega > 0$, while $\Gamma_\pm = \Gamma \pm \sqrt{|\Omega|}$ for $\Omega < 0$. The material quantities are the mass density $\rho \simeq 1$ g cm^{-3}, the layer compression modulus $B \simeq 10^7$–10^8 erg cm^{-3}, the layer bending elastic constant $K \simeq 10^{-6}$ erg cm^{-1}, two combinations of the five characteristic

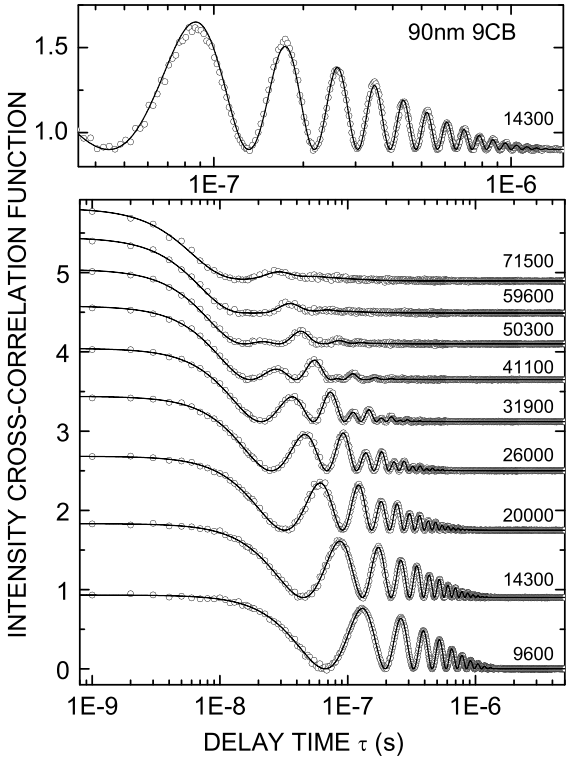

FIG. 1. Measured time correlation functions of the intensity of light scattered from layer undulations in a 90 nm thick smectic-A film of 9CB ≈ 0.5 °C below the nematic phase. Results are shown for various values of the wave vector $q_\perp$ (in cm^{-1}) parallel to the layers, with an estimated uncertainty in $q_\perp$ of ± 300 cm^{-1}. The solid lines are fits to the sum of an underdamped undulation mode and a separate overdamped mode. Top panel: A detail of the oscillating region of a correlation function with 13 resolved peaks. In this case, the solid line is a fit to Eq. (1) of the text for a pure underdamped mode (with parameters $\omega = \sqrt{\Omega}$, Γ, and C_0).

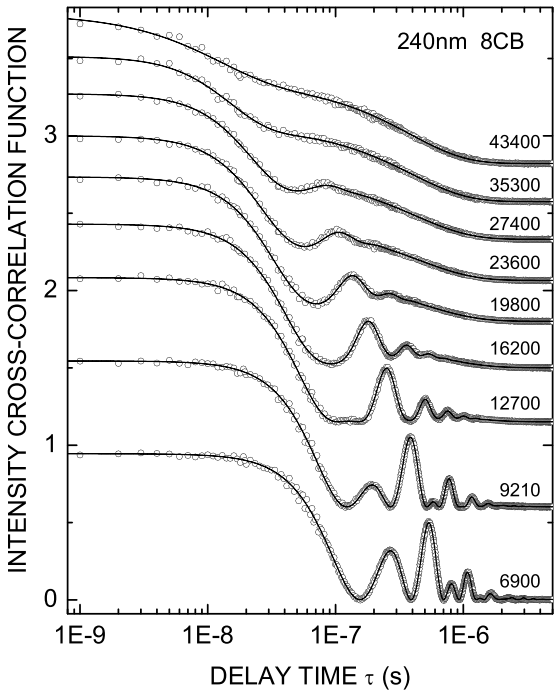

FIG. 2. Intensity time correlation functions measured on a 240 nm thick 8CB film ≈ 7 °C below the smectic-A to nematic transition. The solid lines are fits to a single underdamped undulation mode plus a purely overdamped mode, whose impact is clearly seen at intermediate $q_\perp$ where the oscillations ride on top of the additional mode. (In the top curve, both modes are overdamped.)

viscosities of a smectic-A phase, η_3 and $\eta' = \eta_1 + \eta_2 - 4\eta_3 + \eta_4 - 2\eta_5$ [17], and a length scale $\lambda_P \simeq 10^{-6}$ cm describing molecular permeation between layers. C_0 and $C_\pm$ are $\vec{q}$-dependent amplitudes given in Ref. [10]. When $\Omega > 0$ (i.e., for lower values of $q_\perp$), the $u - v$ modes consist of a pair of counter-propagating "second sound" waves. On the other hand, at sufficiently large $q_\perp$ where $\Omega < 0$, these underdamped modes split into distinct, overdamped elastic and inertial modes (with damping Γ_- and Γ_+, respectively).

For a thin, freestanding smectic film, the dispersion of Γ and Ω are strongly affected by the surface boundary conditions [5,6,9,10], which introduce the surface tension γ of the film in air and the film thickness d. The boundary conditions also quantize the component of the fluctuation wave vector normal to the film, q_z, into discrete branches $\{q_{z,n}: n = 0, 1, 2, \ldots\}$. In principle, the temporal correlations in u contain contributions from all $q_{z,n}$. However, the lowest branch with $n = 0$ and $q_z = q_{z,0}$ should completely dominate our measurements, since it corresponds to undulation of the film with essentially no layer compression for the values of d and $q_\perp$ studied. Quantitatively, when $q_\perp^2 \ll B/(\gamma d) \sim 10^{12}$ cm^{-2}, the value of $q_{z,0}^2$ in the expressions for Γ and Ω is given by $Bq_{z,0}^2 \approx (2\gamma/d)q_\perp^2$ [10], where $q_\perp = (2\pi/\lambda)(\sin\theta_s - \sin\theta_i)$ with θ_i, θ_s representing the laboratory incident and scattering angles (measured from the film normal) and λ denoting the wavelength of light in air. Combining these observations with the theoretical results reviewed above, we then expect to observe a single underdamped mode when $\Omega > 0$, and at least the slower of a pair of relatively fast overdamped modes when $\Omega < 0$, with

$$\Gamma = [\eta_3(1 + 2\gamma/Bd) + \eta'(2\gamma/Bd)/(1 + 2\gamma/Bd) + 2\rho\gamma\lambda_P^2/(\eta_3 d)]q_\perp^2/2\rho + \tilde{\Gamma}q_\perp^4 + O(q_\perp^6) \quad (2)$$

$$\Omega = 2\gamma q_\perp^2/\rho d + \tilde{\Omega}q_\perp^4 - \Gamma^2 + O(q_\perp^6). \quad (3)$$

Here $\tilde{\Gamma}$ and $\tilde{\Omega}$ are coefficients of higher order (quartic) terms in $q_\perp$ dictated by the detailed surface boundary conditions [10].

Now let us compare our correlation data to the prediction of Eq. (1). For light scattering in the homodyne limit, we expect the measured intensity correlation function to be proportional to $C_u^2(\tau)$. Then, as shown by the solid line in the top panel of Fig. 1, Eq. (1a), with three fit parameters ω, Γ, and C_0, provides a good description of data taken on a thin film in the underdamped regime (lower values of $q_\perp$). However, at larger $q_\perp$ and particularly for the thicker film (Fig. 2), we find that a second *purely overdamped* mode, whose presence we already noted, is required to model the data accurately. This mode contributes two more fit parameters (a damping rate and amplitude) for a total of five. At the largest $q_\perp$ in the thicker film, the film undulations pass into the overdamped regime, as expected from Eq. (3) where larger $q_\perp$ and d both tend to drive Ω through zero. In this case, the solid lines in Fig. 2 are fits to the slower of the pair of $u - v$ modes in Eq. (1b) (with parameters C_- and Γ_-) plus the additional overdamped mode, for a total of four parameters. (The faster $u - v$ mode, with damping Γ_+, was not detected.) Thus, the Chen-Jasnow model, supplemented by an overdamped mode of unidentified origin, gives an excellent quantitative description of the data for the full experimental range of $q_\perp$ and d, and thereby allows us to extract the frequency and damping parameters for the film undulation mode. These are plotted for four different films in Fig. 3.

Using Eqs. (2) and (3), we fit the experimentally determined $q_\perp$ dependence of $\omega = \sqrt{\Omega}$ and Γ (underdamped regime) or the value of $\Gamma_- = \Gamma - \sqrt{|\Omega|}$ (overdamped regime). For each film, a single set of four parameters [the coefficients of the $q_\perp^2$ and $q_\perp^4$ terms in Eqs. (2) and (3)] were used to describe both the frequency and damping data over the full range of $q_\perp$. We find that inclusion of the $q_\perp^4$ terms is essential for reasonable fits of the data at large $q_\perp$ (see the solid lines in Fig. 3), particularly as regards the crossover from under- to overdamped behavior observed in the thicker films. The importance of the $q_\perp^4$ terms arises in part because the measured "effective" viscosity,

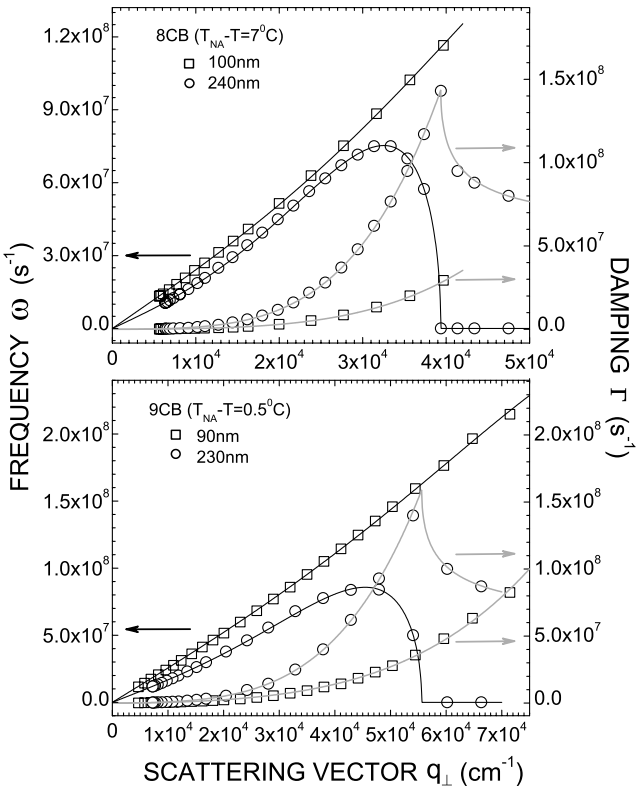

FIG. 3. Dispersion of the frequency and damping for the $n = 0$ undulation mode in four smectic-A films of the compounds and thicknesses indicated. The solid lines are fits based on Eqs. (2) and (3), including $q_\perp^4$ terms. In the thicker films, the crossover to overdamped behavior (where the parameter Ω passes through 0) corresponds to the maxima in the curves for the damping. (Beyond the crossover, we have set the frequency to zero.)

$\eta_{\rm eff} \equiv \lim_{q_\perp \to 0} \Gamma/q_\perp^2$, is quite small. Indeed, from the fits, we find $\eta_{\rm eff} = 0.015$ g cm^{-1} s^{-1} in the thicker films (both materials and temperatures) and roughly 40% lower values in the thinner films. These values are at least 10 times lower than previously reported for single smectic viscosities in bulk samples [11,12]. On the other hand, we find $\gamma = 29$ erg cm^{-2} for the surface tension for all four films, a value that is reasonably consistent with prior results [13]. Finally, we obtain coefficients for the $q_\perp^4$ terms in Eqs. (2) and (3) of order $\tilde{\Gamma} \sim 10^{-12}$–$10^{-11}$ and $\tilde{\Omega} \sim 10^{-3}$ (in cgs units).

To explain the small value of $\eta_{\rm eff}$ and the prominence of the $q_\perp^4$ terms in the measured dispersion, we first consider a scenario involving the bulk viscosities alone. From Eq. (2), we see that $\eta_{\rm eff}$, given by the coefficient of the $q_\perp^2$ term, could be small if $\eta' < 0$. In fact, stability only requires $\eta_3 > 0$ and $\eta' > -4\eta_3$ [17]. Then taking the extreme case $\eta' = -4\eta_3$, Eq. (2) gives $\eta_{\rm eff} = \eta_3[(1 - 2\gamma/Bd)^2/(1 + 2\gamma/Bd)] + 2\rho\gamma\lambda_P^2/(\eta_3 d)$. For $B \simeq 10^7$–10^8 erg/cm^3, $d \simeq 10^{-5}$ cm, and $\gamma = 29$ dyn/cm, the bracketed term can in principle approach zero. Since the permeation contribution is also very small, $\eta_{\rm eff}$ *could* be substantially lower than the individual viscosites. Expanding the simplest form of the surface boundary conditions [5,6,9,10] to $O(q_\perp^4)$ gives the quartic coefficients $\tilde{\Gamma}$ and $\tilde{\Omega}$ as $\tilde{\Gamma} = -\eta'\gamma^2/(12\rho B^2)$ and $\tilde{\Omega} = 2\gamma(\lambda_P^2 - \gamma d/12B)/(\rho d)$. Taking typical magnitudes of the parameters (and again $\eta' = -4\eta_3$), we estimate values of $\tilde{\Gamma}$and $\tilde{\Omega}$ that are both positive (as observed in Fig. 3), but 10–100 times too low in magnitude. Such a large discrepancy suggests a different explanation for our results; namely, the introduction of a distinct surface viscosity [18] for smectic films, to which surface light scattering experiments would be especially sensitive, and a corresponding modification of the boundary conditions. The mechanism and consequences of such a ''dynamic decoupling'' of surface and bulk merit further theoretical investigation. Finally, as to the origin of the additional overdamped mode, we wish at present only to note the following features: that the damping rate of this mode for $q_\perp \geq 10^4$ cm^{-1} is in the MHz range and appears to depend only weakly on $q_\perp$; that the mode is not primarily due to independent optic axis fluctuations, since we detected no depolarized scattering; and that for fixed $q_\perp$ the mode makes a more significant contribution in thicker films.

To summarize, we have applied photon correlation spectroscopy with nanosecond resolution to the study of layer dynamics in smectic-*A* films in the domain where inertia, damping, and elasticity have comparable impacts. While the component of the light scattering correlation function arising from simple film undulations is well described by a hydrodynamic model that assumes incompressibility and constant temperature, several features of our results point to the need for a more complete theoretical analysis of the dynamics of smectic films.

We thank the NSF (DMR99-04321) for support and Professors W. H. de Jeu and N. A. Clark for helpful conversations.

[1] Y. Liao, N. A. Clark, and P. S. Pershan, Phys. Rev. Lett. **30**, 639 (1973).
[2] R. Ribotta, D. Salin, and G. Durand, Phys. Rev. Lett. **32**, 6 (1974).
[3] H. Birecki, R. Schaetzing, F. Rondelez, and J. D. Litster, Phys. Rev. Lett. **36**, 1376 (1976).
[4] These experiments, which utilize electronic spectrum analyzers, have measured the frequency of smectic film undulations up to ~10 MHz, but with no reported results for the damping. [See A. Bottger and J. G. H. Joosten, Europhys. Lett. **4**, 1297 (1987)]. Also, improvements on the spectrum analysis technique have been used to study orientational order fluctuations in isotropic liquid crystals for frequencies between 10 kHz and 1 GHz, but to our knowledge, there have been no applications to smectic membranes. [See T. Masuoka, K. Sakai, and K. Takagi, Phys. Rev. Lett. **71**, 1510 (1993)].
[5] A. Poniewierski, R. Holyst, A. C. Price, L. B. Sorensen, S. D. Kevan, and J. Toner, Phys. Rev. E **58**, 2027 (1998); A. C. Price, L. B. Sorensen, S. D. Kevan, J. Toner, A. Poniewierski, and R. Holyst, Phys. Rev. Lett. **82**, 755 (1999); A. Poniewierski, R. Holyst, A. C. Price, and L. B. Sorensen, Phys. Rev. E **59**, 3048 (1999).
[6] I. Sikharulidze, I. P. Dolbnya, A. Fera, A. Madsen, B. I. Ostrovskii, and W. H. de Jeu, Phys. Rev. Lett. **88**, 115503 (2002); A. Fera, I. P. Dolbnya, G. Grubel, H. G. Muller, B. I. Ostrovskii, A. N. Shalaginov, and W. H. de Jeu, Phys. Rev. Lett. **85**, 2316 (2000).
[7] I. Sikharulidze, B. Farago, I. Dolbnya, A. Madsen, and W. H. de Jeu, Phys. Rev. Lett. **91**, 165504 (2003).
[8] P. G. deGennes and J. Prost, *The Physics of Liquid Crystals* (Clarendon, Oxford, 1993).
[9] A. N. Shalaginov and V. P. Romanov, Phys. Rev. E **48**, 1073 (1993); A. N. Shalaginov and D. E. Sullivan, Phys. Rev. E **62**, 699 (2000).
[10] H.-Y. Chen and D. Jasnow, Phys. Rev. E **61**, 493 (2000); H.-Y. Chen and D. Jasnow, Phys. Rev. E **57**, 5639 (1998).
[11] P. Oswald, J. Phys. (Paris) **47**, 1091 (1986).
[12] C. Baumann, J. P. Marcerou, J. Prost, and J. C. Rouillon, Phys. Rev. Lett. **54**, 1268 (1985).
[13] P. Mach *et al.*, Langmuir **14**, 4330 (1998).
[14] Commercial correlators are also now available with sampling times down to several nsec (see, www.alvgmbh.de and www.correlator.com).
[15] The angular position of the detector corresponding to the specular reflection (and $q_\perp = 0$) was defined by centering the reflection cone on the detector aperture. This was done with an accuracy of $\approx \pm 300$ cm^{-1}.
[16] A. Vrij, J. G. H. Joosten, and H. M. Fijnaut, Adv. Chem. Phys. **48**, 329 (1981).
[17] P. C. Martin, O. Parodi, and P. S. Pershan, Phys. Rev. A **6**, 2401 (1972).
[18] G. E. Durand and E. G. Virga, Phys. Rev. E **59**, 4137 (1999).